Electronic Supplementary Material (ESI) for Journal of Materials Chemistry B.


# Supporting Information

## A Hypoxia-Activatable Theranostic Agent with Intrinsic Endoplasmic Reticulum Affinity and Type-I Photosensitivity

Junqing Zhang, Yongkang Zhang, Hao Zhang, Wenhao Zhai, Xiaoqian Shi, and Changhua Li*

*State Key Laboratory of Medicinal Chemical Biology, College of Pharmacy, and Key Laboratory of Functional Polymer Materials of Ministry of Education, Nankai University, Tianjin 300071, China.*

### 1. Materials and instruments

Unless otherwise noted, reagents were used as received from commercial sources. Solvent preparations were carried according to described procedures.[1] Trypsin-EDTA (0.25%) and 3-(4,5-dimethylthiazol-2-yl)-2,5-diphenyltetrazolium bromide (MTT) were purchased from Invitrogen. Dulbecco's Modified Essential Medium (DMEM), fetal bovine serum (FBS), and 10 × phosphate buffer saline (PBS; pH 7.4) were purchased from Gibco (Life Technologies, AG, Switzerland). 2′,7′-dichlorfluorescein-diacetate (DCF-DA), 1,3-diphenylisobenzofuran (DPBF), rose bengal (RB), dihydroethidium (DHE), aminophenyl fluorescein (APF), coumarin-3-carboxylic acid (3-CCA), and 5,5-dimethyl-1-pyrroline-*N*-oxide (DMPO) were purchased from Sigma-Aldrich. Water was deionized with a Milli-Q SP reagent water system (Millipore) to a specific resistivity of 18.2 MΩcm. 4-(3-Phenyltzobenzofuryl)phenyl trimethylammonium iodide (QDPBF)[2] and 4-hydroxy-3,5-diiodo-benzaldehyde[3] were synthesized according to literature methods.

$^{1}$H and $^{13}$C NMR spectra were recorded at 25 °C on a Bruker AV400 NMR spectrometer, operating at 400 and 100 MHz, respectively, where chemical shifts ($\delta$ in ppm) were determined using partially or non-deuterated solvent residues as internal references. DMSO-$d_6$ and $CDCl_3$ were used as the solvents. High-resolution mass spectra (HRMS) were obtained on Varian 7.0T FTMS. HPLC analysis were performed with a Shimadzu HPLC system, equipped with a LC-20AT binary pump, an SPD-20A UV-vis detector, and a Symmetry C18 column. Dynamic light scattering (DLS) studies were performed using a Zetasizer NanoZS (Malvern). Morphological analyses were conducted on transmission electron microscopy (TEM; Talos L120C G2, FEI). UV-visible absorption spectra were recorded on a UH5300 double-beam UV-Vis spectrophotometer (Hitachi). Fluorescence spectra were recorded on an F-4600 (Hitachi) spectrofluorometer. MTT assay were monitored by the microplate reader (SpectraMax i3x, MD). Cells fluorescence images were obtained using an inverted fluorescence microscope (ZOE Fluorescent Cell imager, BIO-RAD). Confocal laser scanning microscopy (CLSM) images were acquired using a Leica TCS SP8 microscope. In Vivo Fluorescence imaging of tumor-bearing mice were conducted on NightOWL II LB983 In Vivo Imaging System (Berthold Technologies).

## 2. Preparation and characterization of $^{ER}$PS@NP, Im@NP, and Nb@NP.

### 2.1 Preparation of nanoparticles

A 0.4 mL of THF solution of F127 (10 mg) and PS (**$^{ER}$PS**, **$^{ER}$PSIm**, or **$^{ER}$PSNb**; 200 nmol) was slowly dropped into 10 mL deionized water under stirring at 500 rpm at room temperature. The resulting solution was stirred overnight under this condition, led to most of the THF be evaporated. Residual THF was removed under reduced pressure, and an appropriate amount of water was added to obtain a stock aqueous solution of nanoparticle of **$^{ER}$PS@NP**, **Im@NP**, or **Nb@NP** (conc. 20 $\mu$M PS). **Im@NP** solution with a higher concentration for in vivo experiment can be readily prepared via concentrating the stock solution by ultrafiltration.

### 2.2 DLS sizing and morphological analysis

*Dynamic light scattering (DLS).* For particle size and polydispersity index (PDI) measurement, the stock solutions were 5-fold diluted with deionized water and passed through a 0.45 $\mu$m filter. Measurements were made in triplicate at 25 °C using Zetasizer NanoZS. Zetasizer Nano software (version 7.12) was used to analyze the data.

*Transmission electron microscopy (TEM).* The samples were prepared by dropping 10 $\mu$L sample solution onto a carbon-film-coated copper grid, the grid was air-dried before imaging. TEM observations were conducted on a Talos L120C-G2 electron microscope at an acceleration voltage of 120 kV.

### 2.3 Stability studies.

UV-vis absorption spectrophotometer and dynamic light scattering (DLS) study were adopted to evaluate the spectral and colloidal stability of **$^{ER}$PS@NP**, respectively. The UV-vis absorption spectrum and size distribution of **$^{ER}$PS@NP** were recorded over a period of 48 h.

### 2.4 p$K_a$ Determination

The p$K_a$ value of the **$^{ER}$PS** molecule embedded in **$^{ER}$PS@NP** was determined using the Henderson-Hasselbalch equation:[4]

$$\log[(A_{max} - A)/(A - A_{min})] = pK_a - pH \qquad (S1)$$

where $A_{max}$ and $A_{min}$ represent maximum absorbance and minimal absorbance at the measured wavelength, respectively, A represents the observed absorbance. The p$K_a$ values (p$K_a$ = 5.63) were then calculated based on the plots of $\log[(A_{max} - A)/(A - A_{min})]$ *vs.* pH as shown in Figure S2.

### 2.5 Fluorescence quantum yield ($\Phi_{fl}$) determination

According to a previous report,[5] $\Phi_{fl}$ of the **$^{ER}$PS** molecule embedded in **$^{ER}$PS@NP** was measured using rhodamine B as a reference with fluorescence quantum yield ($\Phi_{fl}$) of 0.97 in ethanol.[6] The fluorescence quantum yield ($\Phi_{fl}$) was calculated by using the following formula:

$$\Phi_X = \Phi_{ST}\left(\frac{Grad_X}{Grad_{ST}}\right)\left(\frac{\eta_X^2}{\eta_{ST}^2}\right) \qquad (S2)$$

where $\Phi_X$ and $\Phi_{ST}$ are the fluorescence quantum yields of the sample and the standard (rhodamine B), respectively, $Grad_X$ and $Grad_{ST}$ are the gradients from the plots of the integrated fluorescence intensity vs absorbance of the sample and rhodamine B, respectively. The absorbance of the sample or rhodamine B at the excitation wavelength was less than 0.1. $\eta_X$ and $\eta_{ST}$ are the refractive indices of the solvents used for the sample and rhodamine B, respectively. UV-vis absorption spectra were recorded on a UH5300 double-beam UV-Vis spectrophotometer (Hitachi). Fluorescence spectra were recorded on a F-4600 (Hitachi) spectrofluorometer. Measurements were carried out in 1 cm quartz

cuvettes with a total sample volume of 3 mL.

### 3. Detection of photosensitized ROS generation in solution

#### 3.1 General ROS detection in solution

The total photogenerated ROSs by **$^{ER}$PS@NP** was measured using QDPBF as a probe.[7] Typically, the stock aqueous solution of QDPBF was added to the aqueous solution of **$^{ER}$PS@NP** to give a final aqueous test solution (conc. 2.5 $\mu$M **$^{ER}$PS**). For the QDPBF content, it was fixed at a concentration where the absorbance at 415 nm is around 1.0. The obtained solutions were then placed in a cuvette and subjected to light irradiation (Xe lamp, 490-700 nm, 2 mW/cm$^2$) for 120 s. The change in absorbance of QDPBF (ΔAbs) at 415 nm was recorded at 10-s intervals to evaluate the photosensitivity in producing ROS. $\Delta Abs = Abs_0 - Abs_t$; where $Abs_0$ and $Abs_t$ are the absorbance of QDPBF at 415 nm before and after light irradiation, respectively.

#### 3.2 Singlet oxygen ($^1O_2$) detection.

The $^1O_2$ generated by **$^{ER}$PS@NP** upon light irradiation was measured using ABDA as an indicator.[8] Typically, the stock aqueous solution of ABDA was added to the PBS solution of **$^{ER}$PS@NP** to give a final aqueous test solution (conc. 2.5 $\mu$M **$^{ER}$PS**). For the ABDA content, it was fixed at a concentration where the absorbance at 380 nm is around 1.0. The obtained solutions were then placed in a cuvette and subjected to light irradiation (Xe lamp, 490-700 nm, 5 mW/cm$^2$) for 10 min. The decrease in absorbance of ABDA (ΔAbs) at 380 nm was recorded at 2-min intervals to evaluate the photosensitivity in producing $^1O_2$. $\Delta Abs = Abs_0 - Abs_t$; where $Abs_0$ and $Abs_t$ are the absorbance of ABDA at 380 nm before and after light irradiation, respectively.

#### 3.3 Superoxide anion radical ($O_2^{\bullet-}$) detection.

The photogenerated $O_2^{\bullet-}$ by **$^{ER}$PS@NP** was measured using DHE as a fluorescence probe with the aid of DNA-*ct*.[9] Typically, the stock solution of DHE and aqueous solution of DNA-*ct* were sequentially added to the PBS solution of **$^{ER}$PS@NP** to give a final aqueous test solution (conc. 2.5 $\mu$M **$^{ER}$PS**, 10 $\mu$M DHE, 40 $\mu$g/mL DNA-*ct*). The obtained solutions were then placed in a cuvette and subjected to light irradiation (Xe lamp, 490-700 nm, 2 mW/cm$^2$) for 10 min. The fluorescence emission spectrum was recorded at 2-min intervals. The fluorescence intensity enhancement of DHE at 580 nm (ΔFlu) was calculated to evaluate the photosensitivity in producing $O_2^{\bullet-}$. $\Delta Flu = Flu_t - Flu_0$; where $Flu_0$ and $Flu_t$ represent the emission intensities of DHE at 580 nm in the presence of photosensitizers before and after light irradiation, respectively.

#### 3.4 Detection of photosensitized ROS generation via EPR spectrometry

Electron paramagnetic resonance (EPR) spectra were recorded on a Bruker EMXplus 6/1 EPR spectrometer. 5,5-Dimethyl-1-pyrroline-*N*-oxide (DMPO) was used as a special radical trapping agent for superoxide anions ($O_2^{\bullet-}$).[11] Briefly,100 mM DMPO was mixed with 100 $\mu$M **$^{ER}$PS** in DMSO (containing 0.1% TX-100), followed by light irradiation (LED lamp, 520±10 nm, 5 mW/cm$^2$) for 3 min. EPR was then performed at a microwave frequency of 9.8 GHz and power of 20 mW with a modulation amplitude and frequency of 1.0 G and 100 kHz, respectively, time constant 0.01 ms, scan time 30 s, receiver gain 30 dB, and center field setting 3512 G.

### 4. Biological studies

#### 4.1 Cell culture

*Cell culture under normoxic conditions (21% $O_2$).* HeLa and 4T1 cell lines were purchased from American Type Culture Collection (ATCC). Cells were cultured in culture media (HeLa cells: DMEM; 4T1 cells: DME/F-12) supplemented with 10% heatinactivated FBS, penicillin (100 U/mL), and strepotomycin (100 $\mu$g/mL) in a 37 °C incubator with 5% $CO_2$. Before experiment, the cells were pre-cultured until confluence was reached to about 75%.

*Cell culture under hypoxic conditions (0.1% $O_2$).* To simulate the hypoxic tumor environment, HeLa cells were incubated under hypoxia. Briefly, after incubation under normoxic conditions (21% $O_2$), the cells were transferred to a hypoxia incubator chamber (Stemcell Technologies), and incubated for additional 24 h at 37 °C in a humidified atmosphere (0.1% $O_2$, 5% $CO_2$, and 94.9% $N_2$). The oxygen content in the chamber was being monitored using an oxygen detector (Nuvair, $O_2$ Qucikstick). Before experiment, the cells were pre-cultured until confluence was reached to about 75%.

**4.2 Colocalization studies**

Colocalization studies of **$^{ER}$PS@NP** in HeLa cells was studied using different organelle fluorescent trackers (endoplasmic reticulum: ER-Tracker Green; mitochondria: Mito-Tracker Green; lysosome: Lyso-Tracker Green). HeLa cells were cultured in confocal imaging dishes at 37 ºC. After 70% confluence, the culture medium was removed and washed twice with PBS. After incubation with **$^{ER}$PS@NP** (2 $\mu$M) for 4 h, the cells were washed twice with PBS. Then, freshly prepared organelle fluorescent tracker (ER-Tracker Green: 1 $\mu$M; Mito-Tracker Green: 200 nM; Lyso-Tracker Green: 200 nM) in DMEM was added and the cells were incubated for another 30 min. The cells were then imaged immediately by confocal laser scanning microscope (CLSM). Red channel of **$^{ER}$PS@NP** was at 600-750 nm with excitation at 561 nm. Green channel of trackers was at 500-540 nm with excitation at 488 nm.

**4.3 Intracellular NTR-responsiveness of Im@NP** or **Nb@NP**

HeLa cells were divided into two groups: group 1, incubated with **Im@NP** (2 $\mu$M **$^{ER}$PSIm**) under normoxia for 24 h; group 2, incubated with **Im@NP** (2 $\mu$M **$^{ER}$PSIm**) under hypoxia for 24 h. After washing with PBS (10 mM, pH 7.4) for three times, the cells of different groups were imaged immediately by CLSM. Notably, for experiments in hypoxia, cell culture and treatments were conducted in a hypoxia incubator chamber, and all the DMEM used were bubbled with mixed gas (0.1% $O_2$, 5% $CO_2$, and 94.9% $N_2$) for 5 min in advance. Ex/Em: 561/600-750 nm. The intracellular NTR-responsiveness of **Nb@NP** was also performed following the same procedure as described above.

**4.4 Intracellular total ROS determination with DCF-DA.**

Dichlorofluorescein diacetate (DCF-DA) was chosen as an oxidant-sensitive fluorescent dye to detect the formed ROS, which rapidly oxidized DCF-DA into highly fluorescent dichlorofluorescein (DCF).[12] Typically, HeLa cells were incubated with **$^{ER}$PS@NP** (2 $\mu$M **$^{ER}$PS**) under normoxic or hypoxic conditions for 24 h, the cells were washed thrice with PBS (10 mM, pH 7.4), freshly prepared DCF-DA solution (20 $\mu$M) in DMEM was added and the cells were incubated for 0.5 h. The cells were washed with PBS (10 mM, pH 7.4), then subjected to light irradiation (Xe lamp, 490-700 nm, 5 mW/cm$^2$) for 5 min, and imaged immediately on an inverted fluorescence microscope. Notably, for experiments in hypoxia, cell culture and treatments were conducted in a hypoxia incubator chamber, and all the DMEM used were bubbled with mixed gas (0.1% $O_2$, 5% $CO_2$, and 94.9% $N_2$) for 5 min in advance.

**4.5 Intracellular $O_2^{\bullet-}$ Determination with DHE.**

DHE was used as a specific fluorescent dye to detect the generated $O_2^{\bullet-}$. Typically, HeLa cells were incubated with **$^{ER}$PS@NP** (2 $\mu$M **$^{ER}$PS**) or **Im@NP** (2 $\mu$M **$^{ER}$PSIm**) under normoxia or hypoxia for 24 h, the cells were washed twice with PBS (10 mM, pH 7.4), freshly prepared DHE solution (20 $\mu$M) in DMEM was added and the cells were incubated for 20 min. The cells were washed with PBS (10 mM, pH 7.4), then subjected to light irradiation (Xe lamp, 490-700 nm, 10 mW/cm$^2$) for 2 min, and imaged immediately by CLSM. Ex/Em: 561/570-600 nm. Notably, for experiments in hypoxia, cell culture and treatments were conducted in a hypoxia incubator chamber, and all the DMEM used were bubbled with mixed gas (0.1% $O_2$, 5% $CO_2$, and 94.9% $N_2$) for 5 min in advance.

**4.6 Intracellular •OH Determination with 3-CCA.**

Coumarin-3-carboxylic acid (3-CCA) was chosen as an oxidant-sensitive fluorescent dye to detect the formed •OH, which rapidly oxidized 3-CCA into highly fluorescent 7-hydroxylcoumarin-3-carboxylic acid.[13] Typically, HeLa cells were incubated with **$^{ER}$PS@NP** (2 $\mu$M **$^{ER}$PS**) or **Im@NP** (2 $\mu$M **$^{ER}$PSIm**) under normoxia or hypoxia for 24 h, the cells were washed twice with PBS (10 mM, pH 7.4), freshly prepared 3-CCA solution (20 $\mu$M) in DMEM was added and the cells were incubated for another 20 min. The cells were washed with PBS (10 mM, pH 7.4), then subjected to light irradiation (Xe lamp, 490-700 nm, 10 mW/cm$^2$) for 10 min, and imaged immediately by CLSM. Ex/Em: 405/410-460 nm. Notably, for experiments in hypoxia, cell culture and treatments were conducted in a hypoxia incubator chamber, and all the DMEM used were bubbled with mixed gas (0.1% $O_2$, 5% $CO_2$, and 94.9% $N_2$) for 5 min in advance.

**4.7 Live/dead staining**

HeLa cells were incubated with **$^{ER}$PS@NP** (2 $\mu$M **$^{ER}$PS**) or **Im@NP** (2 $\mu$M **$^{ER}$PSIm**) under normoxia (21% $O_2$) or hypoxia (0.1% $O_2$) for 24 h. Cells were washed twice with PBS, then subjected to light irradiation (Xe lamp, 490-700 nm, 5 mW/cm$^2$) for 10 min and incubated for additional 12 h (**$^{ER}$PS@NP**) or 36 h (**Im@NP**). After washing with PBS, the cells were stained with Calcein AM (1.5 $\mu$M) and propidium iodide (PI, 6.0 $\mu$M). After staining for 30 min, the cells were washed with PBS (10 mM, pH 7.4) and imaged immediately on an inverted fluorescence microscope. Notably, for experiments in hypoxia, cell culture and treatments were conducted in a hypoxia incubator chamber, and all the DMEM used were bubbled with mixed gas (0.1% $O_2$, 5% $CO_2$, and 94.9% $N_2$) for 5 min in advance.

**4.8 MTT assa*y*.**

HeLa cells were seeded in 96-well plates at an initial density of ca. $1 \times 10^4$ cells per well, and incubated under normoxia (21% $O_2$) or hypoxia (0.1% $O_2$). Then, HeLa cells were incubated with **$^{ER}$PS@NP** or **Im@NP** of varying concentrations of dye components for 24 h, the cells were washed with PBS and subjected to light irradiation (Xe lamp, 490-700 nm, 5 mW/cm$^2$) for 10 min. After 36 h incubation, freshly prepared MTT solution (20 $\mu$L, 5 mg/mL) in culture medium was added into each well. The cells were further incubated for 4 h at 37 °C. The MTT medium in each well was then carefully removed and replaced by DMSO (150 $\mu$L). The plate was gently agitated to dissolve all the precipitates formed. The absorbance at 490 nm was monitored by the microplate reader (SpectraMax i3x, MD).

## 5. Supplementary figures

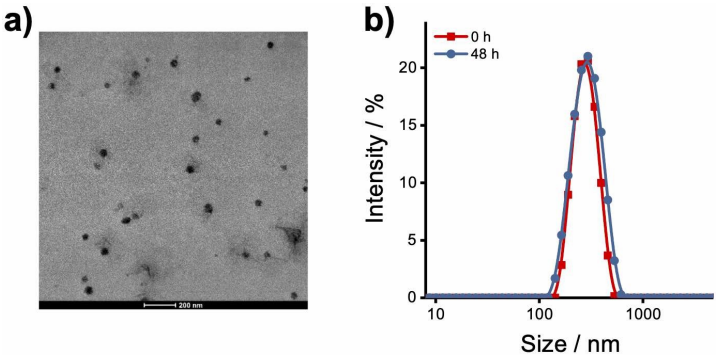


**Figure S1.** (a) Typical TEM image of $^{ER}$**PS@NP**; scale bar is 200 nm. (b) Size distribution recorded for freshly prepared and aged $^{ER}$**PS@NP** in PBS using dynamic light scattering (DLS) at 25 °C.

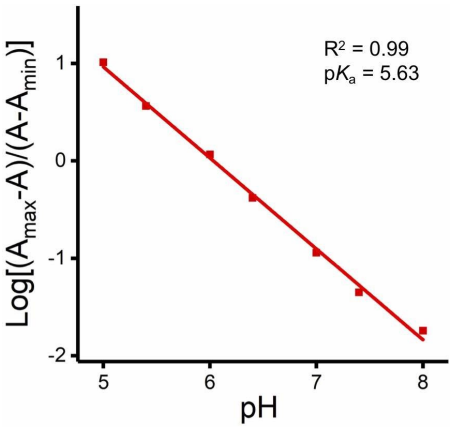


**Figure S2.** Linear fitted curve of log[($A_{max}$ - A)/(A - $A_{min}$)] versus pH value for $^{ER}$**PS@NP**.

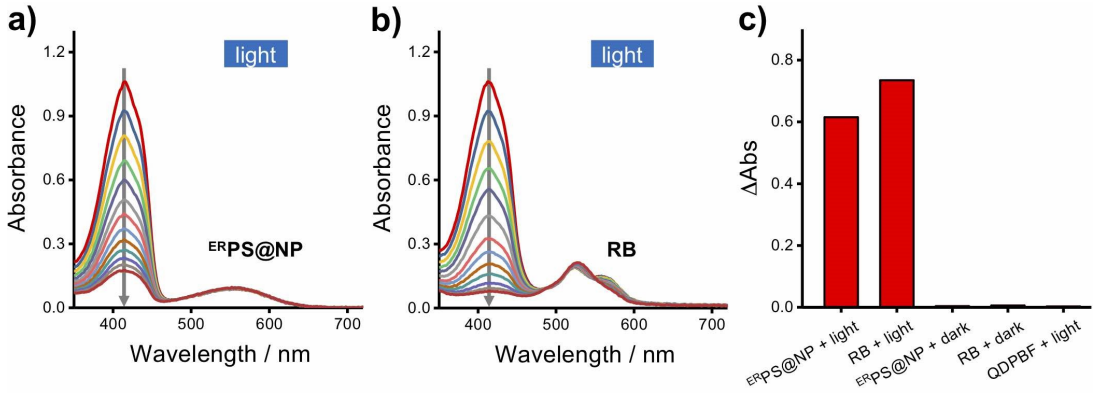


**Figure S3.** Time-dependent UV-vis absorption spectra of QDPBF within aqueous solution of $^{ER}$**PS@NP** (2.5 $\mu$M $^{ER}$**PS**) or RB (2.5 $\mu$M) upon light irradiation for varying time intervals (0-120 s). (c) ΔAbs of QDPBF at 412 nm in the presence of $^{ER}$**PS@NP** or RB after different treatments as indicated (light irradiation for 120 s or dark). Light: Xe lamp (490-700 nm, 2 mW/cm$^2$).

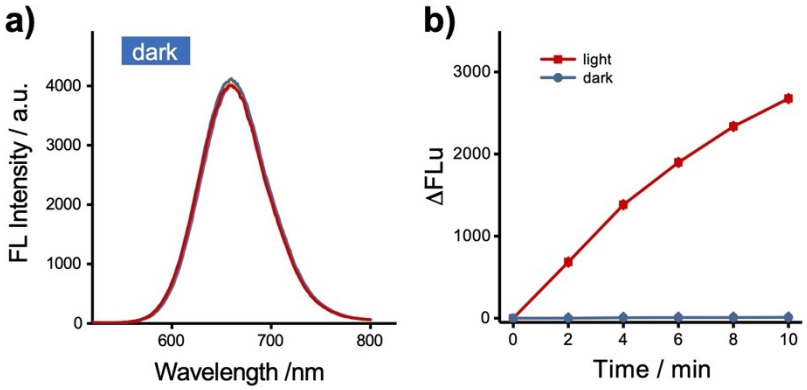


**Figure S4.** (a) Time-dependent fluorescence emission spectra of DHE within aqueous solution of **$^{ER}$PS@NP** (2.5 $\mu$M **$^{ER}$PS**) in dark. (b) Time-dependent fluorescence emission enhancement of DHE at 580 nm (ΔFlu) upon different treatments as indicated (n = 3). Light: Xe lamp (490-700 nm, 2 mW/cm$^2$).

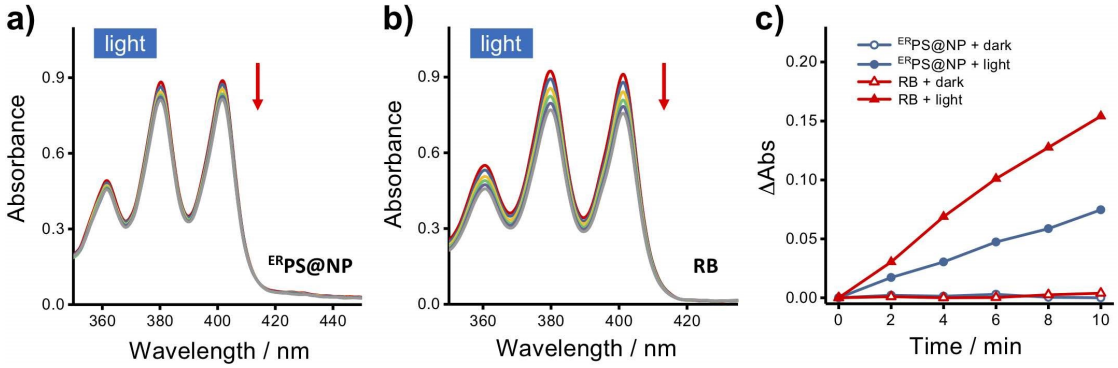


**Figure S5.** Time-dependent UV-vis absorption spectra of ABDA within aqueous solution of **$^{ER}$PS@NP** (2.5 $\mu$M **$^{ER}$PS**) or RB (2.5 $\mu$M) upon light irradiation for varying time intervals (0-10 min). (c) ΔAbs of ABDA at 380 nm in the presence of **$^{ER}$PS@NP** or RB after different treatments as indicated (light irradiation for 10 min or dark). Light: Xe lamp (490-700 nm, 5 mW/cm$^2$).

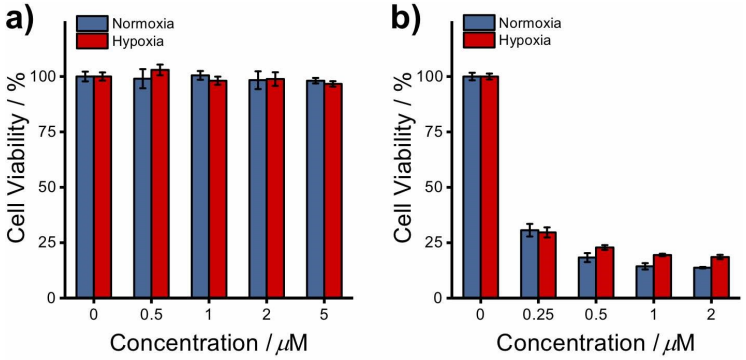


**Figure S6.** Cell viability of HeLa cells incubated with **$^{ER}$PS@NP** of indicated concentrations of **$^{ER}$PS** component under normoxia or hypoxia in dark (a) or upon light irradiation (b) determined by MTT assay (n = 4). Light: Xe lamp (490-700 nm, 5 mW/cm$^2$, 10 min).

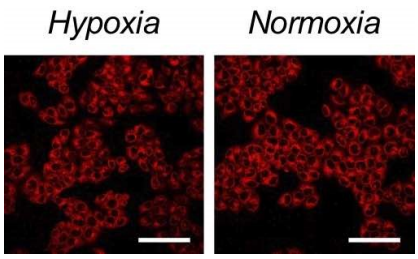


**Figure S7.** Cell uptake of $^{ER}$**PS@NP** by HeLa cells in normoxia and hypoxia environment. Scale bar: 100 $\mu$m.

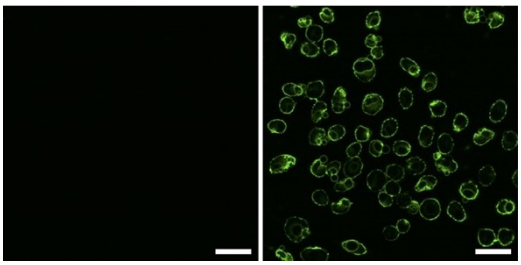

**Figure S8.** Confocal fluorescence imaging of the apoptosis of $^{ER}$**PS@NP**-incubated HeLa cells without (left) and with (right) light irradiation using Annexin V-FITC as a fluorescent indicator. Scale bar: 50 $\mu$m.

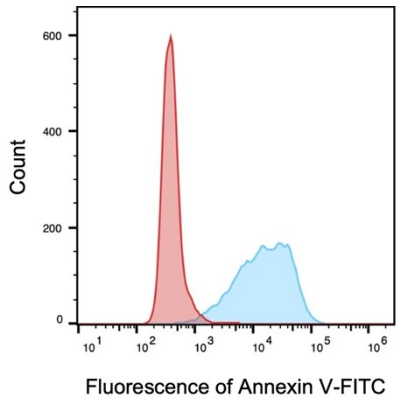


**Figure S9.** Flow cytometry analysis of the apoptosis of $^{ER}$**PS@NP**-incubated HeLa cells without (red) and with (cyan) light irradiation using Annexin V-FITC as a fluorescent indicator.

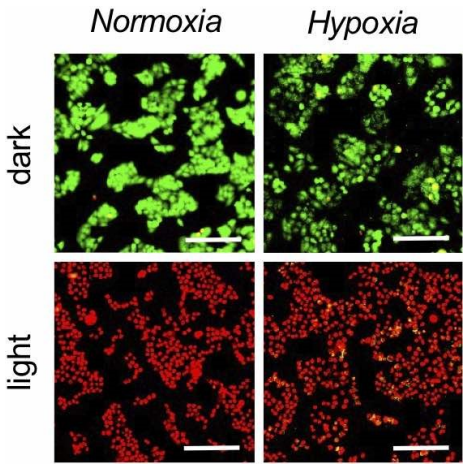


**Figure S10.** Live/dead staining images of HeLa cells treated with $^{ER}$**PS@NP** (2.0 $\mu$M $^{ER}$**PS**) under normoxia or hypoxia. Scale bar: 200 $\mu$m. Light: Xe lamp (490-700 nm, 5 mW/cm$^2$, 10 min).

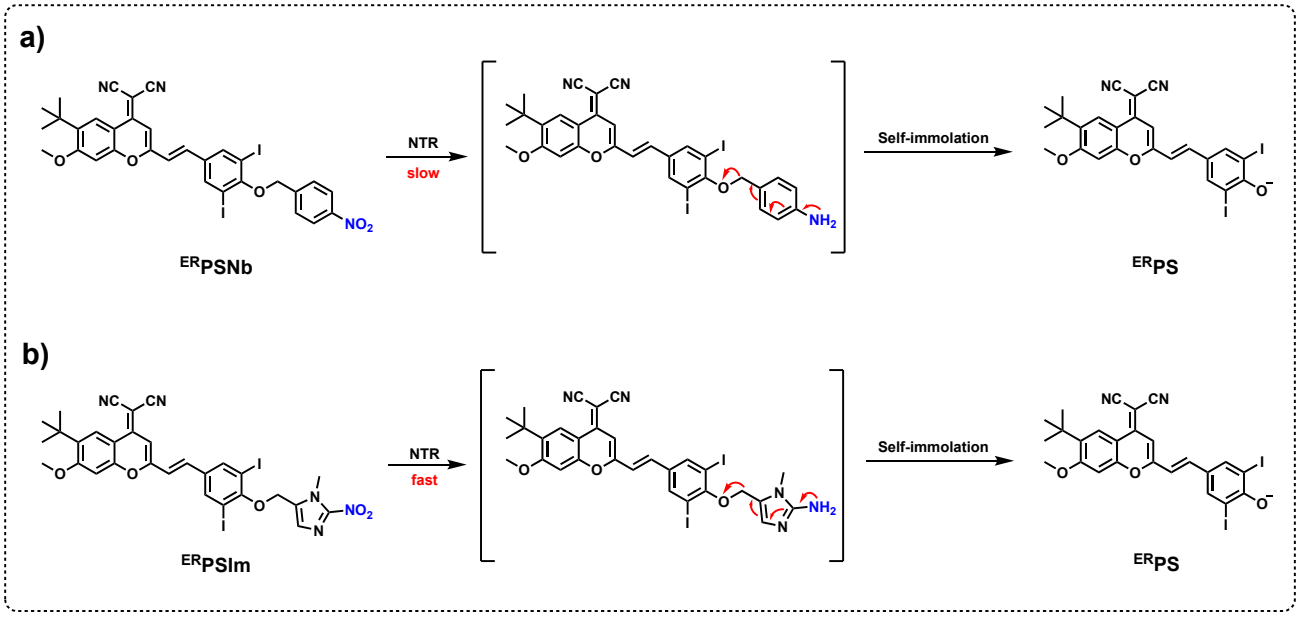


**Scheme S1.** NTR induced reduction of (a) $^{ER}$**PSNb** and (b) $^{ER}$**PSIm** under hypoxic condition.

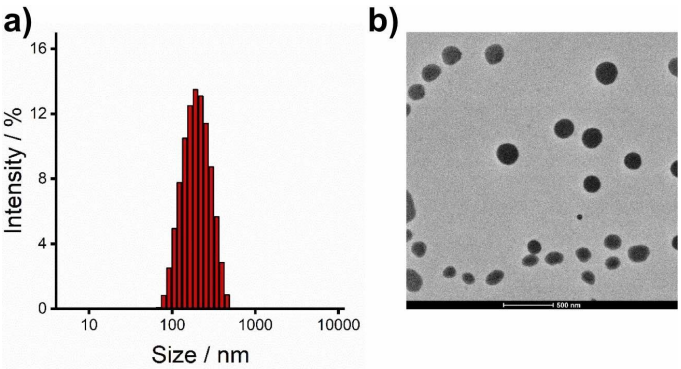

**Figure S11.** (a) Size distribution and (b) typical TEM image of **Nb@NP**. Scale bar: 500 nm.

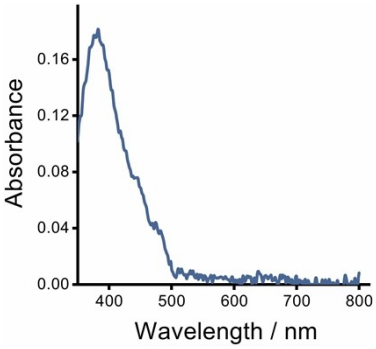


**Figure S12.** UV-vis absorption spectra of **Nb@NP** (~10 $\mu$M $^{ER}$**PSNb**) in PBS at 25 °C

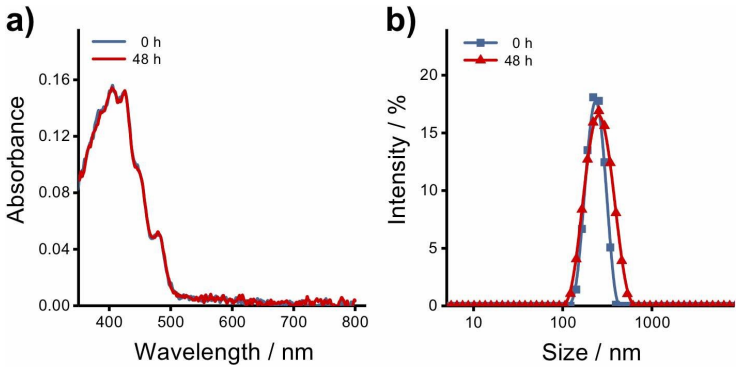


**Figure S13.** (a) Time-dependent UV-vis absorption spectra of **Im@NP** (~10 $\mu$M $^{ER}$**PSIm**) in PBS at 25 °C. (b) Size distribution recorded for freshly prepared and aged **Im@NP** in PBS using dynamic light scattering (DLS) at 25 °C.

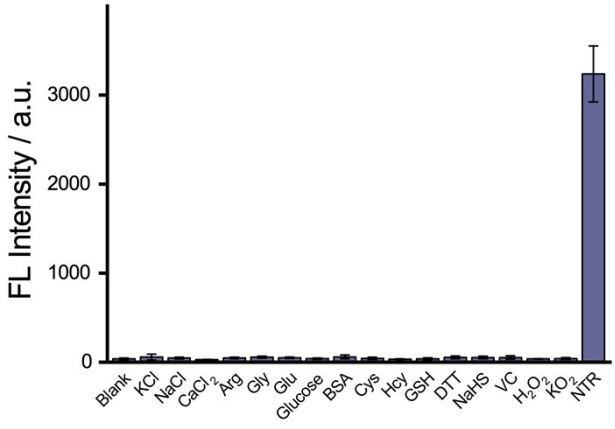


**Figure S14.** Fluorescence emission intensity at 660 nm of **Im@NP** in the presence of different kinds of species, blank (**Im@NP** + NADH), and with KCl (50 mM), NaCl (50 mM), $CaCl_2$ (50 mM), arginine (Arg, 1 mM), glycine (Gly, 1 mM), glutamic acid (Glu, 1 mM), glucose (10 mM), BSA (10 mg/mL), Cys (1 mM), HCy (1 mM), GSH (5 mM), DTT (1 mM), NaHS (1 mM), VC (1 mM), $H_2O_2$ (1 mM), $KO_2$ (1 mM), and NTR (0.2 $\mu$g/mL).

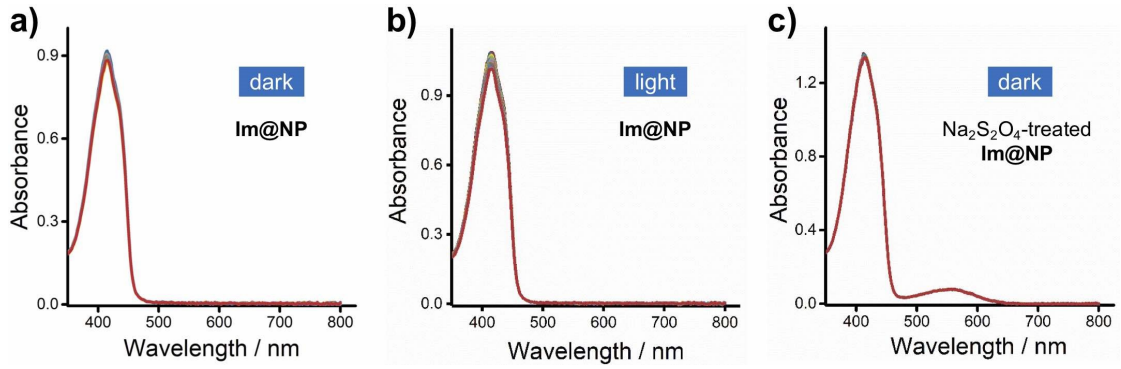


**Figure S15.** (a,b) Time-dependent UV-vis absorption spectra of QDPBF within aqueous solution of **Im@NP** (2.5 $\mu$M **$^{ER}$PSIm**) in dark (a) or upon light irradiation (b) for varying time intervals (0-120 s). (c) Time-dependent UV-vis absorption spectra of QDPBF within aqueous solution of $Na_2S_2O_4$-treated **Im@NP** (2.5 $\mu$M **$^{ER}$PSIm**) in dark. Light: Xe lamp (490-700 nm, 2 mW/cm$^2$).

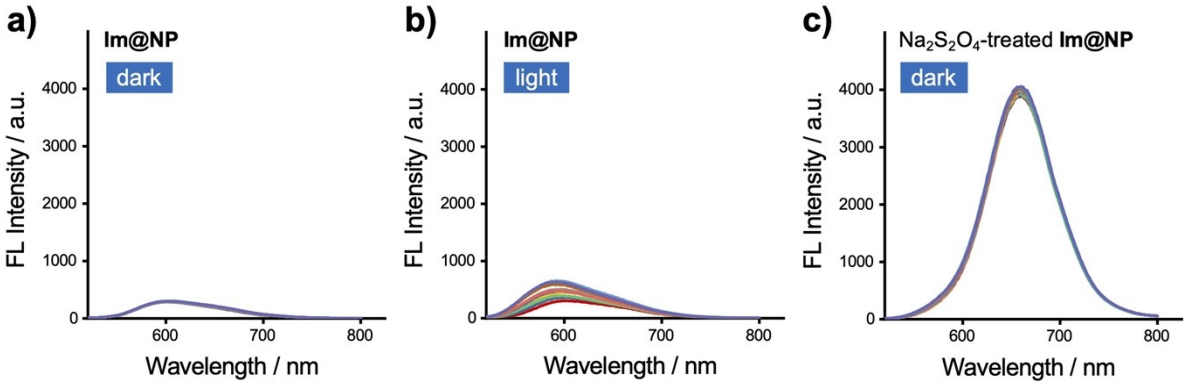


**Figure S16.** (a,b) Time-dependent fluorescence emission spectra of DHE within aqueous solution of **Im@NP** (2.5 $\mu$M **$^{ER}$PSIm**) in dark (a) or upon light irradiation (b) for varying time intervals (0-10 min). (c) Time-dependent fluorescence emission spectra of DHE within aqueous solution of $Na_2S_2O_4$-treated **Im@NP** (2.5 $\mu$M **$^{ER}$PSIm**) in dark. Light: Xe lamp (490-700 nm, 5 mW/cm$^2$).

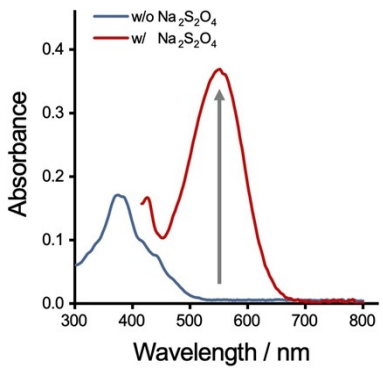


**Figure S17.** UV-vis absorption spectra of **Im@NP** (10 $\mu$M **$^{ER}$PSIm**) before and after $Na_2S_2O_4$ treatment in aqueous media.

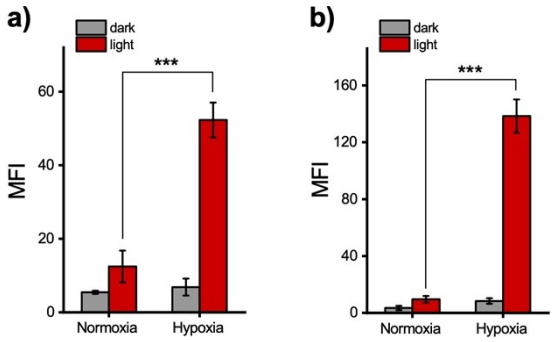


**Figure S18.** Mean fluorescence intensities (MFI) quantified from the CLSM images of Figure 4d (n = 3). (a) DHE fluorescence images. (b) 3-CCA fluorescence images. ***P < 0.001 determined by Student's t-test.

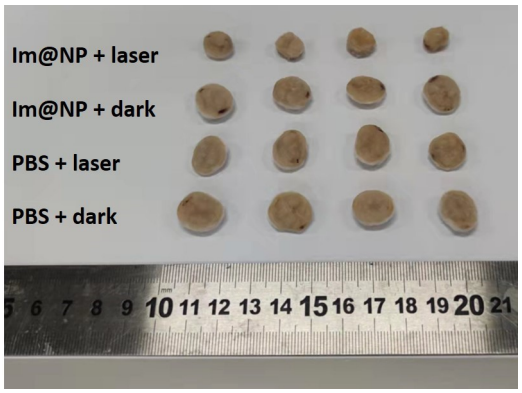


**Figure S19.** Photographs recorded for stark tumors collected after two weeks of observation.

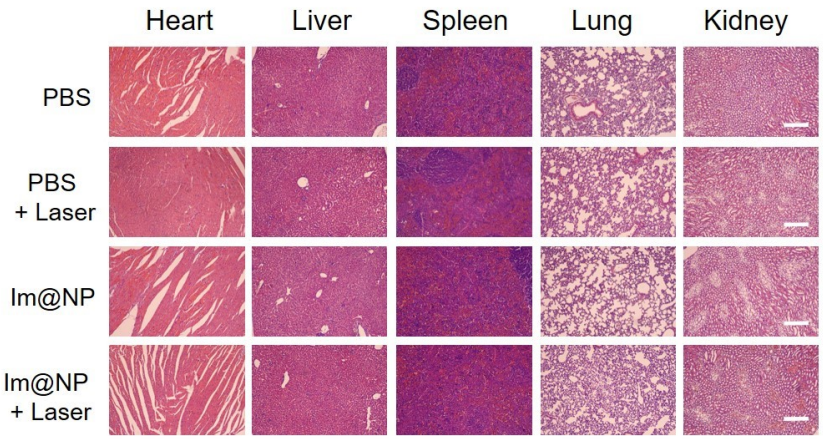


**Figure S20.** H&E staining images of major organs (heart, liver, spleen, lung, and kidney) retrieved from mice in different treatment groups after two weeks of observation. Scale bar: 200 $\mu$m.

**6. NMR and HRMS spectra.**

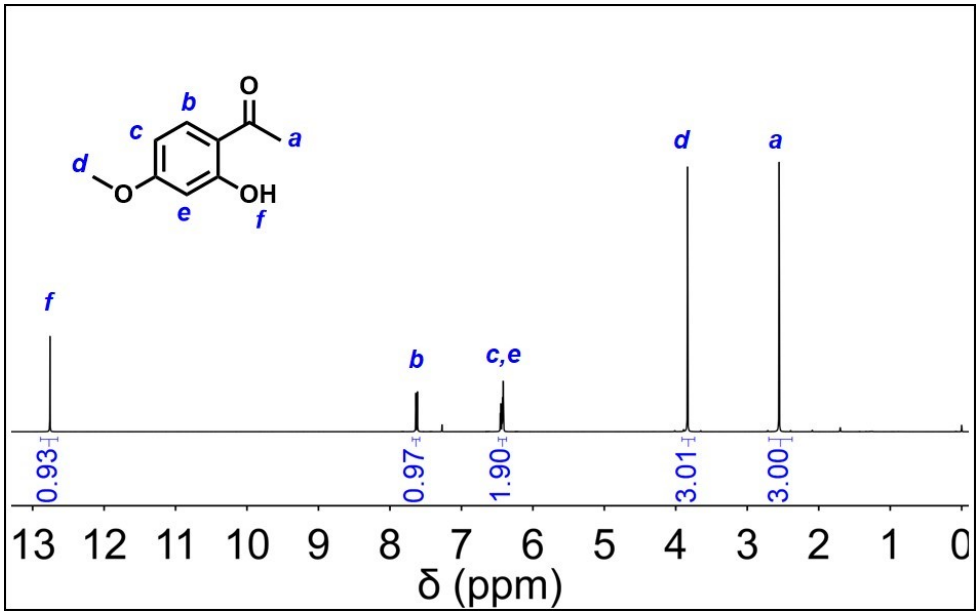


**Figure S21.** $^{1}H$ NMR spectrum (400 MHz) of compound **1** in $CDCl_3$ at 25 ºC.

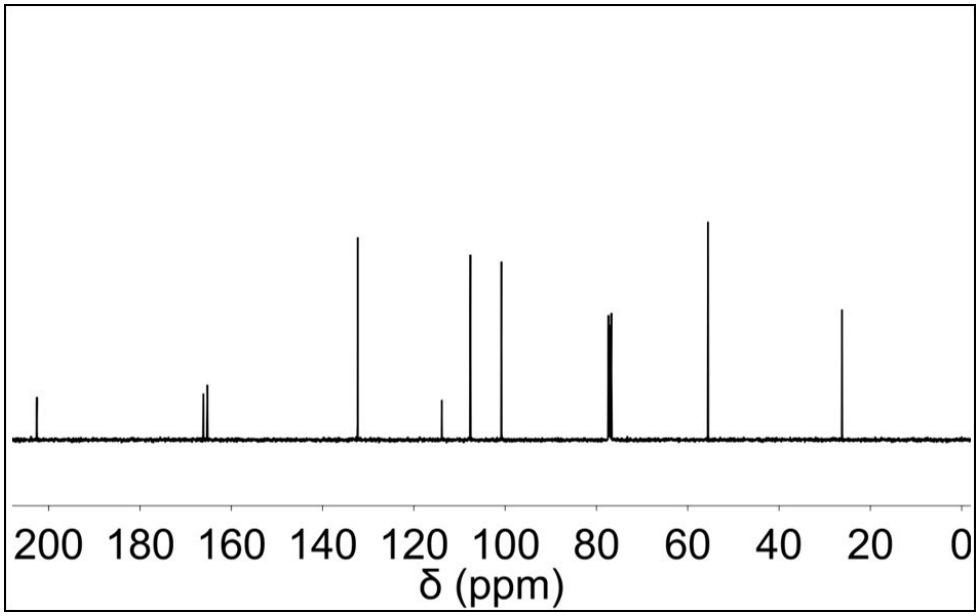


**Figure S22.** $^{13}C$ NMR spectrum (100 MHz) of compound **1** in $CDCl_3$ at 25 ºC.

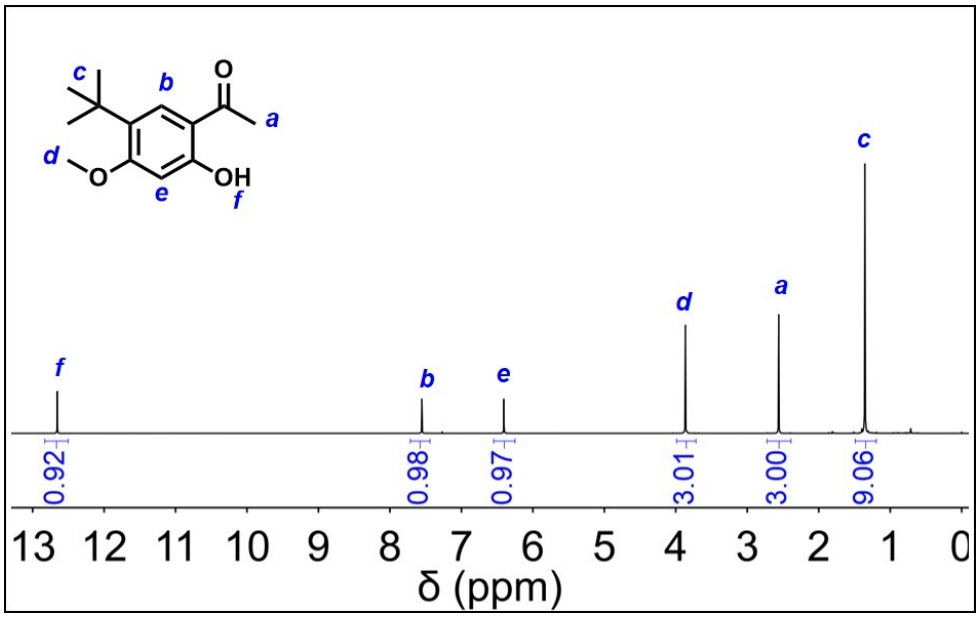


**Figure S23.** $^{1}$H NMR spectrum (400 MHz) of compound **2** in $CDCl_3$ at 25 ºC.

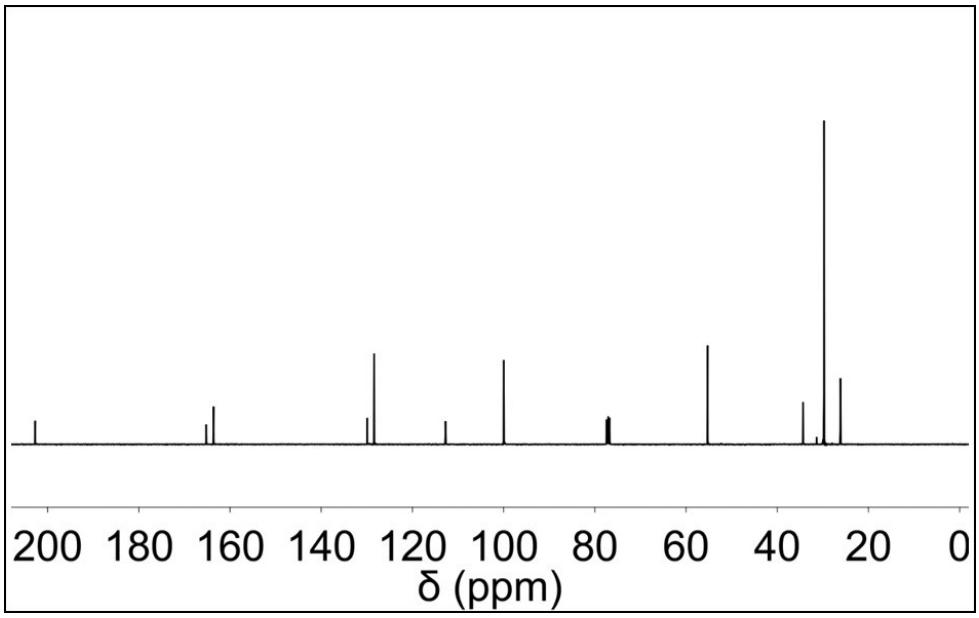


**Figure S24.** $^{13}$C NMR spectrum (100 MHz) of compound **2** in $CDCl_3$ at 25 ºC.

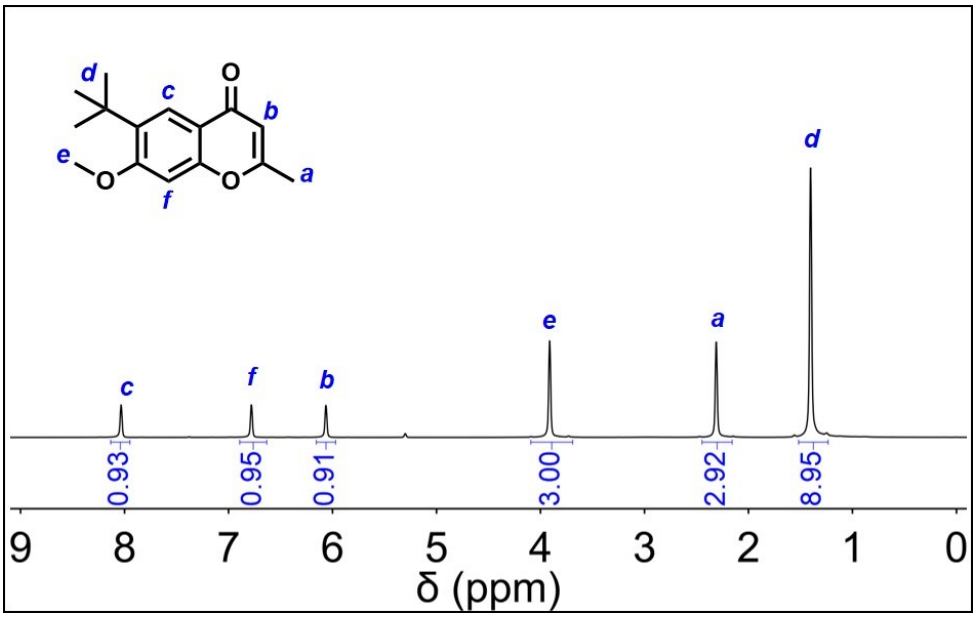


**Figure S25.** $^{1}$H NMR spectrum (400 MHz) of compound **3** in $CDCl_3$ at 25 ºC.

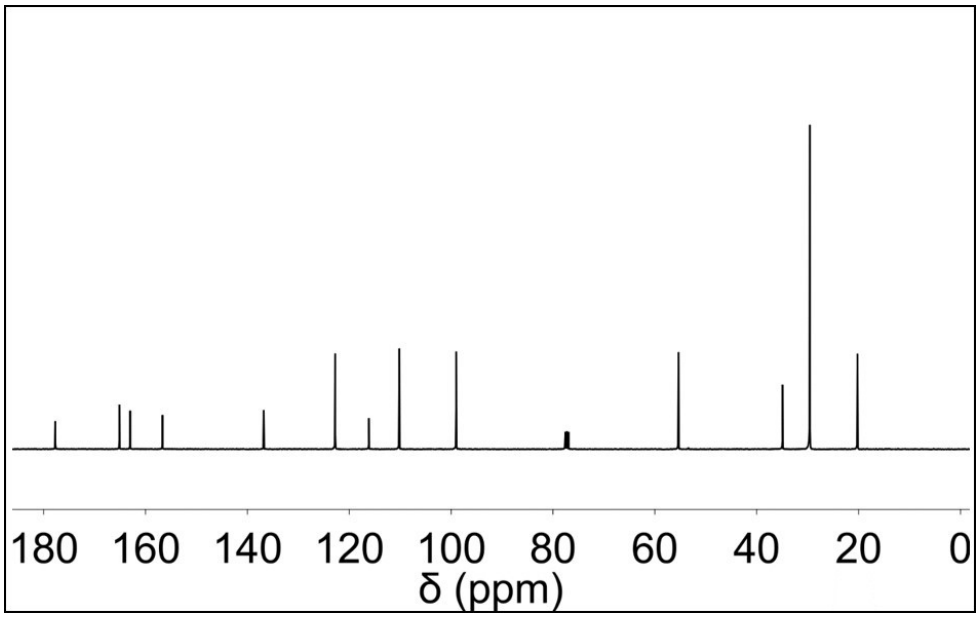


**Figure S26.** $^{13}$C NMR spectrum (100 MHz) of compound **3** in $CDCl_3$ at 25 ºC.

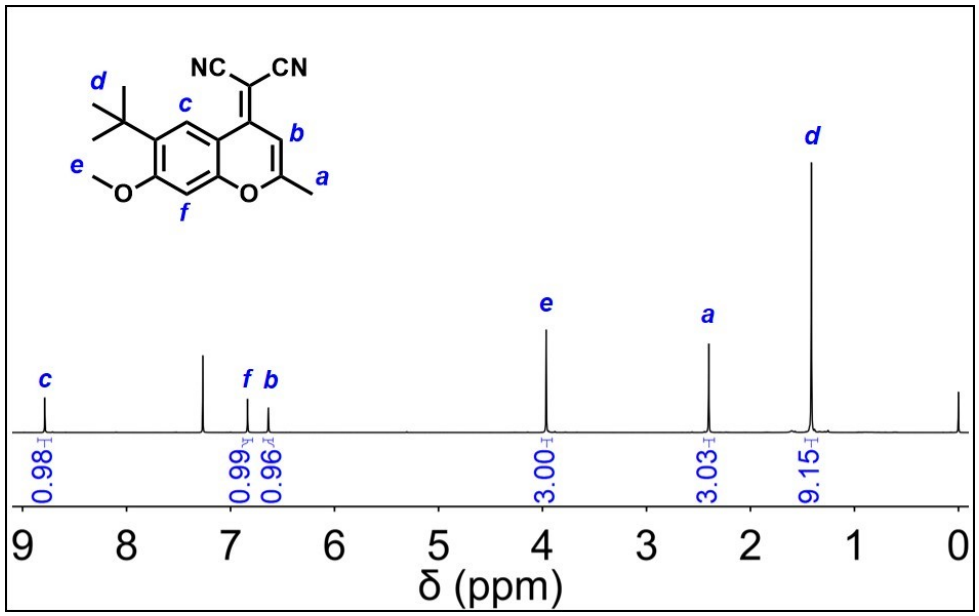


**Figure S27.** $^{1}$H NMR spectrum (400 MHz) of compound **4** in $CDCl_3$ at 25 °C.

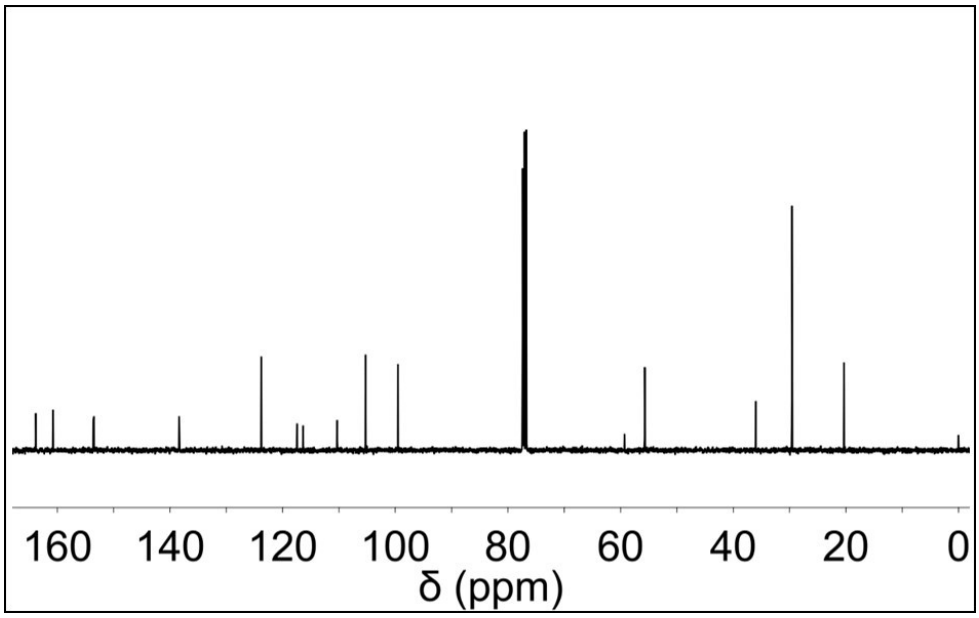


**Figure S28.** $^{13}$C NMR spectrum (100 MHz) of compound **4** in $CDCl_3$ at 25 °C.

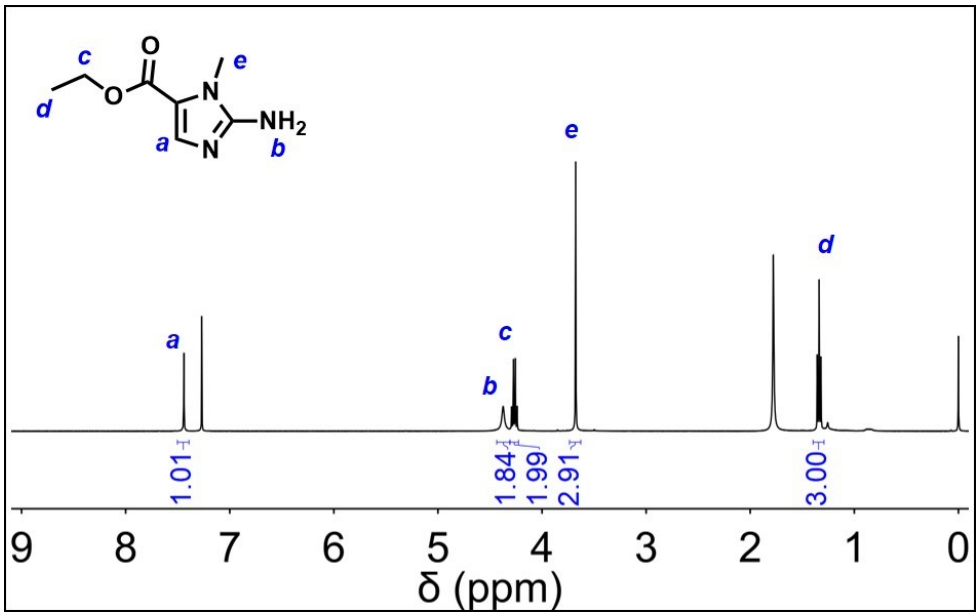


**Figure S29.** [1]H NMR spectrum (400 MHz) of compound **5** in DMSO-$d_6$ at 25 ºC.

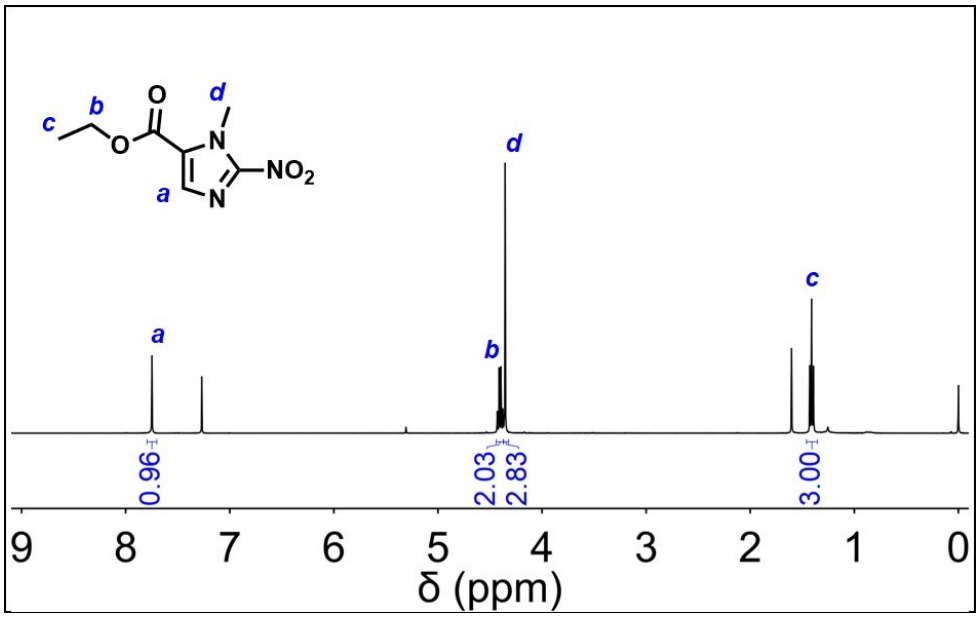


**Figure S30.** [1]H NMR spectrum (400 MHz) of compound **6** in $CDCl_3$ at 25 ºC.

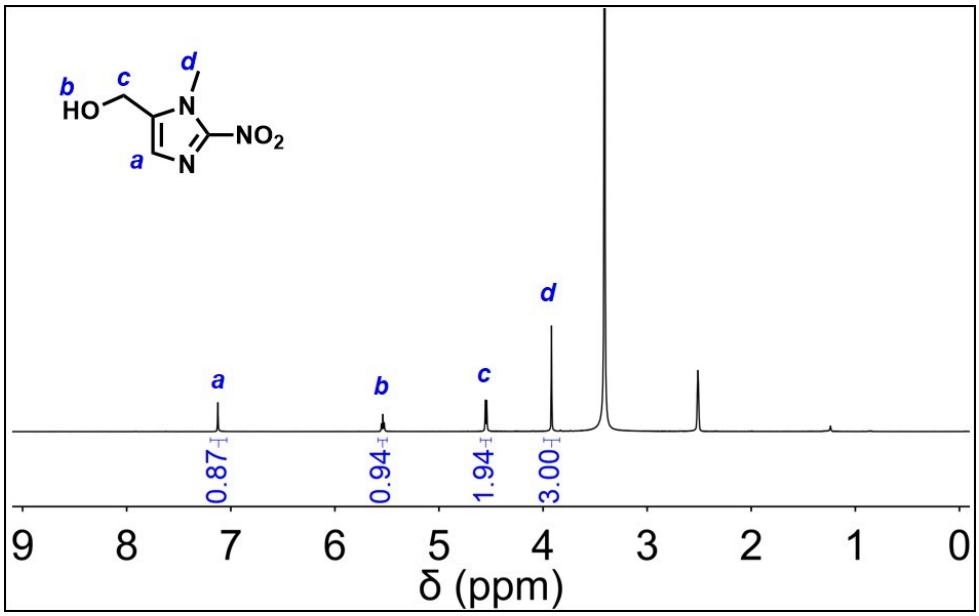


**Figure S31.** [1]H NMR spectrum (400 MHz) of compound **7** in DMSO-$d_6$ at 25 ºC

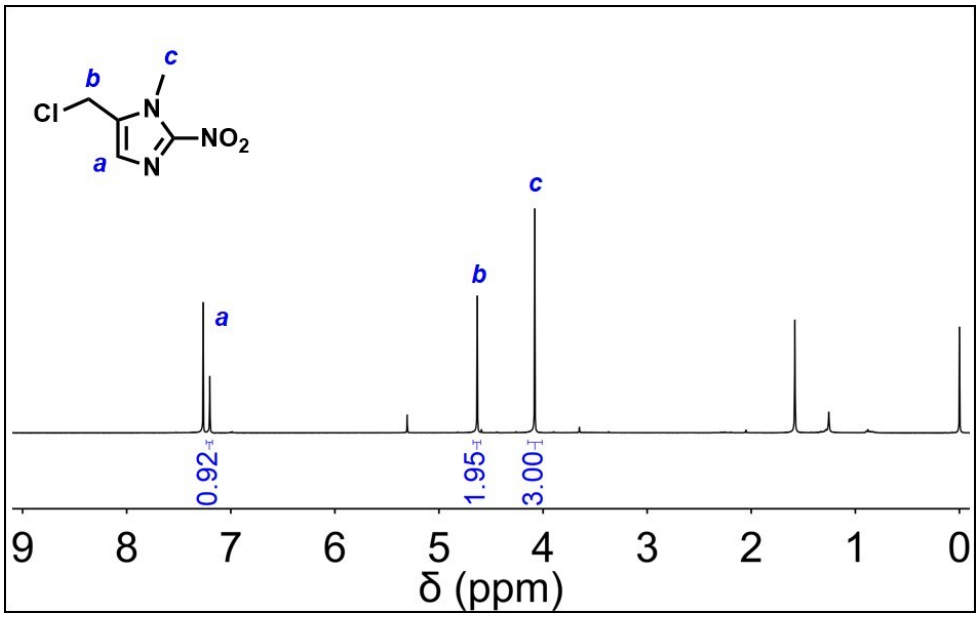


**Figure S32.** [1]H NMR spectrum (400 MHz) of compound **8** in $CDCl_3$ at 25 ºC

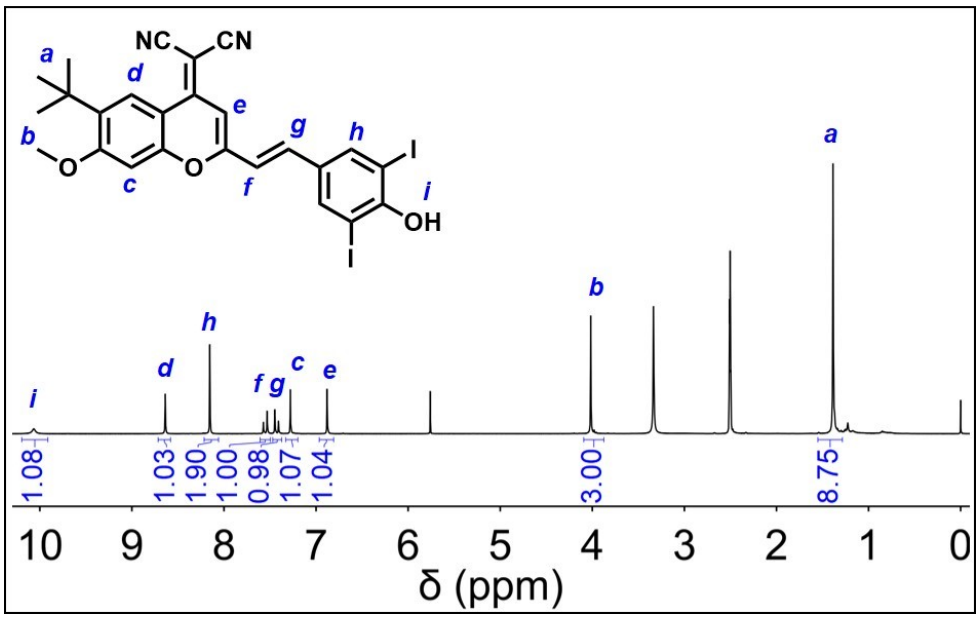


**Figure S33.** $^{1}$H NMR spectrum (400 MHz) of **$^{ER}$PS** in DMSO-$d_6$ at 25 ºC.

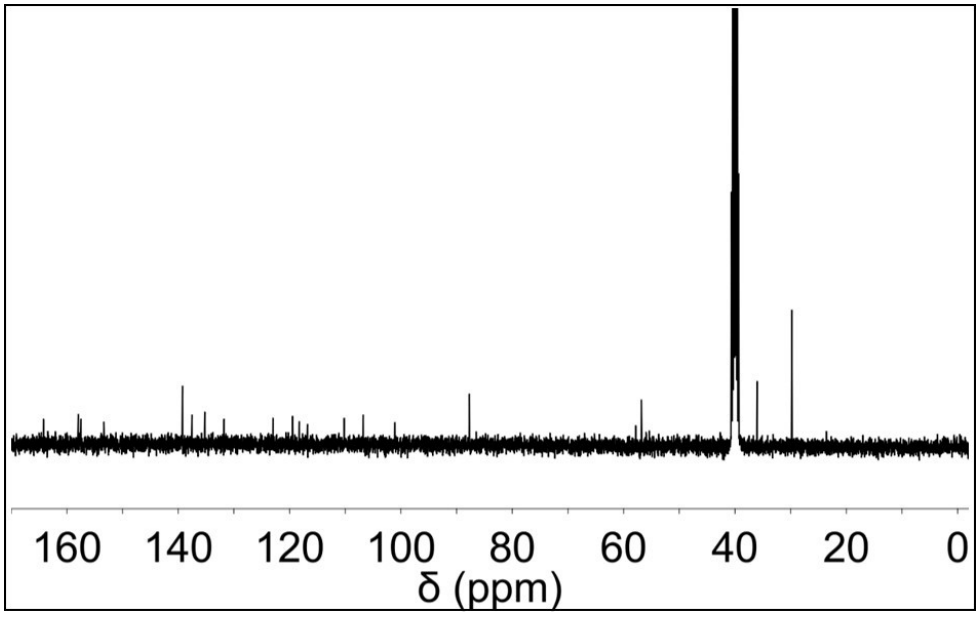


**Figure S34.** $^{13}$C NMR spectrum (100 MHz) of **$^{ER}$PS** in DMSO-$d_6$ at 25 ºC.

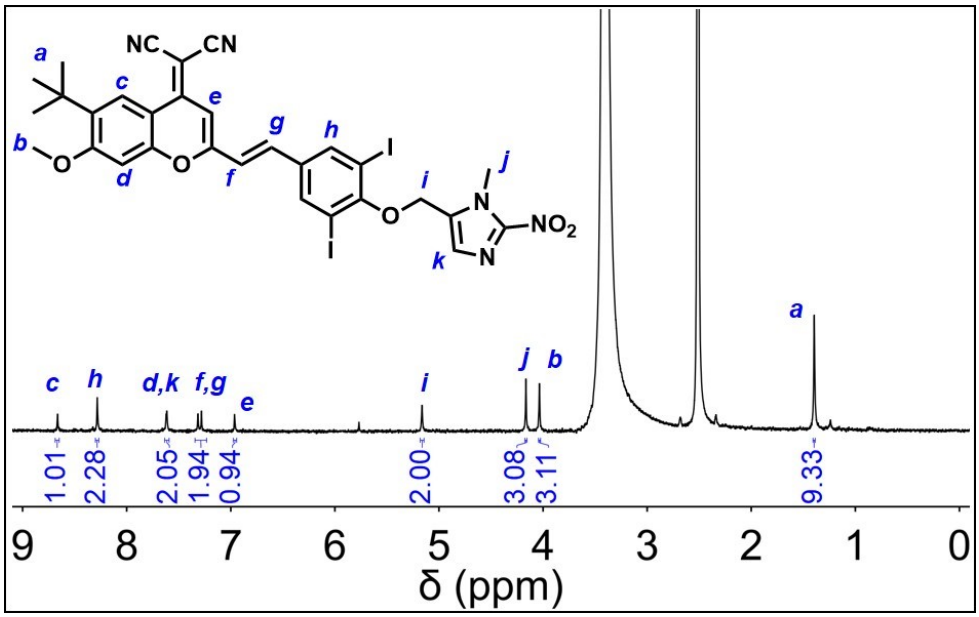


**Figure S35.** $^{1}$H NMR spectrum (400 MHz) of $^{ER}$**PSIm** in DMSO-$d_6$ at 25 ºC.

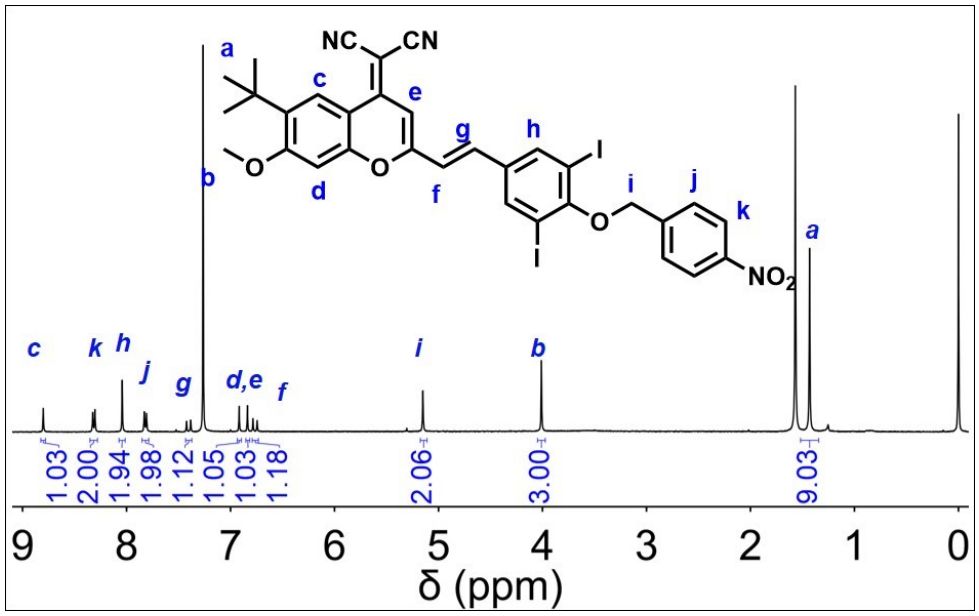


**Figure S36.** $^{1}$H NMR spectrum (400 MHz) of $^{ER}$**PSNb** in $CDCl_3$ at 25 ºC.

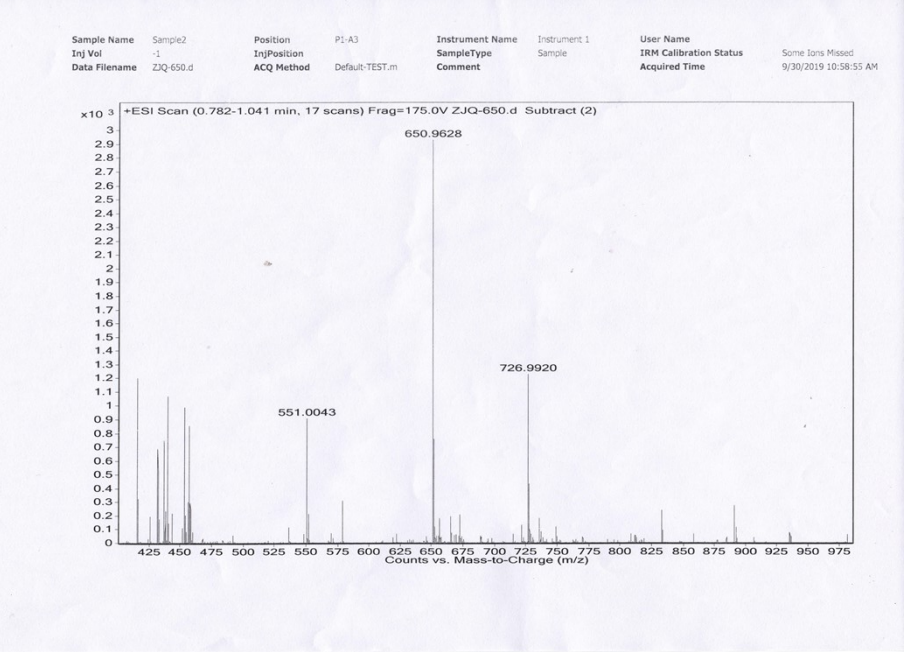


**Figure S37.** HRMS of $^{ER}$**PS**.

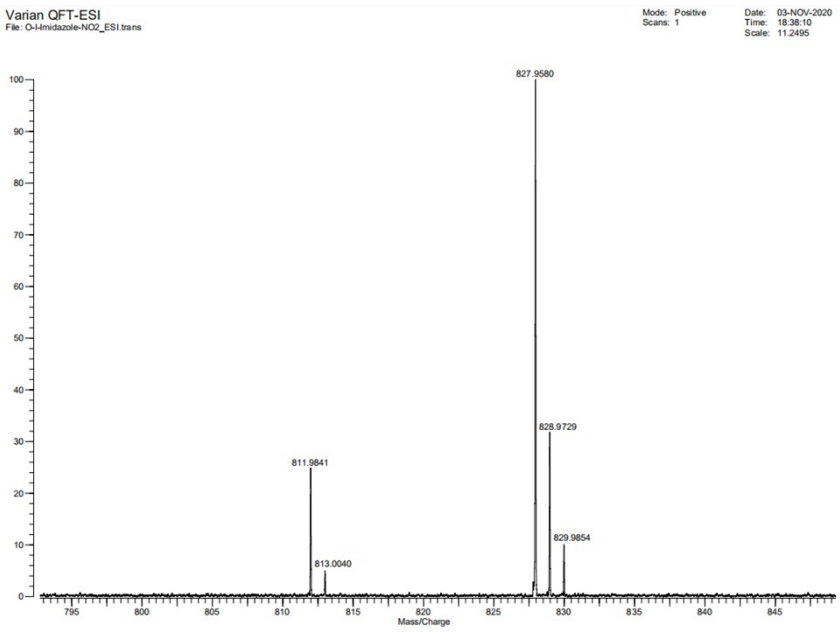

**Figure S38.** HRMS of $^{ER}$**PSIm**.

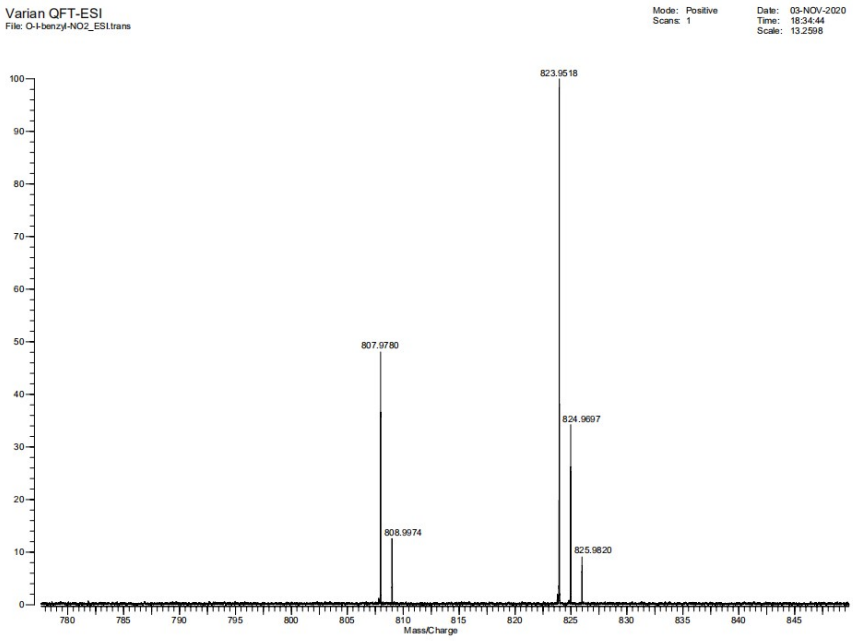


**Figure S39.** HRMS of $^{ER}$**PSNb**.

## 7. References


(1) Armarego, W. L. F.; Perrin, D. D. Purification of Laboratory Chemicals, Butterworth-Heinemann, **2000**.

(2) Amat-Guerri, F.; Lempe, E.; Lissi, E. A.; Rodriguez, F. J.; Trull, F. R. *J. Photoch. Photobio*. **1996**, *A 93*, 49–56.

(3) Emmanuvel, L.; Shukla, R. K.; Sudalai, A.; Gurunath, S.; Sivaram, S. *Tetrahedron Lett*. **2006**, *47*, 4793–4796.

(4) Li, M.; Wu, X. M.; Wang, Y.; Li, Y. S.; Zhu, W. H.; James, T. D. *Chem. Commun*. **2014**, *50*, 1751–1753.

(5) Zheng, H. Z.; Wang, Q. L.; Long, Y. J.; Zhang, H. J.; Huang, X. X.; Zhu, R. *Chem. Commun*. **2011**, *47*, 10650–10652.

(6) Kenmoku, S.; Urano, Y.; Kojima, H.; Nagano, T. *J. Am. Chem. Soc*. **2007**, *129*, 7313–7318.

(7) Kwon, S.; Lee, Y.; Jung, Y.; Kim, J. H.; Baek, B.; Lim, B.; Lee, J.; Kim, I.; Lee, J. *Eur. J. Med. Chem*. **2018**, *148*, 116−127.

(8) Campu, A.; Focsan, M.; Lerouge, F.; Borlan, R.; Tie, L.; Rugina, D.; Astilean, S. *Colloids Surf. B.* **2020**, *194*, 111213.

(9) Zhao, Y. Y.; Zhang, L.; Chen, Z. X.; Zheng, B. Y.; Ke, M. R.; Li, X. S.; Huang, J. D. *J. Am. Chem. Soc*. **2021**, *143*, 13980−13989.

(10) Li, L. Q.; Shao, C.; Liu, T.; Chao, Z. C.; Chen, H. L.; Xiao, F.; He, H. M.; Wei, Z. X.; Zhu, Y. L.; Wang, H.; Zhang, X. D.; Wen, Y. T.; Yang, B.; He, F.; Tian, L. L. *Adv. Mater*. **2020**, *32*, 2003471.

(11) Ding, H. Y.; Yu, H. J.; Dong, Y.; Tian, R. H.; Huang, G.; Boothman, D. A.; Sumer, B. D.; Gao, J. M. *J Control Release*. **2011**, *156*, 276–280.

(12) Feng, L. N.; Li, C. B.; Liu, L. X.; Wang, Z. Y.; Chen, Z. H.; Yu, J.; Ji, W. W.; Jiang, G. Y.; Zhang, P. F.; Wang, J. G.; Tang, B. Z. *ACS Nano*, **2022**, *16*, 4162–4174.

(13) Lan, G. X.; Ni, K. Y.; Veroneau, S. S.; Feng, X. Y.; Nash, G. T.; Luo, T. K.; Xu, Z. W.; Lin, W. B. *J. Am. Chem. Soc*. **2019**, *141*,

4204−4208.